biology

MDPI

Article

Novel Eel Skin Fibroblast Cell Line: Bridging Adherent and Suspension Growth for Aquatic Applications Including Virus Susceptibility

Zaiyu Zheng [1], Bin Chen [1], Xiaodong Liu [1], Rui Guo [2], Hongshu Chi [1], Xiuxia Chen [1], Ying Pan [1] and Hui Gong [1,*]

[1] Biotechnology Institute, Fujian Academy of Agricultural Sciences, Fuzhou 350003, China; cammy_zh@hotmail.com (Z.Z.); chenbinbin0721@163.com (B.C.); xdliu777@163.com (X.L.); chihongshu@faas.cn (H.C.); xiuxiachen@163.com (X.C.); py19860220@sina.com (Y.P.)

[2] Fuzhou Ocean and Fisheries Technology Center, Fuzhou 350007, China

* Correspondence: ghxfjm@163.com; Tel.: +86-0591-87817514

Simple Summary: The adherent and suspension cell culture methods have their own advantages. Adherent culture involves both straightforward steps and inexpensive consumables, and the even spread of cells on the substrate facilitates clear observation of the cell morphology, growth status, and cytopathic effects using a microscope. By comparison, the ability to form a high-density cell population and the ease of scaling up make suspension culture valuable for industrial production, such as vaccine development, bio-pharmaceutical manufacture, medicine screening, and food production. However, very few cell lines can grow in suspension naturally, and the typical commercially used suspension cell culture systems are all mammalian in origin, making them not suitable for a lot of aquatic cases. To meet the needs of aquatic industries, a new ES culture system of aquatic origin was developed through explant outgrowth and enzyme-digesting passaging. The ES cells can adapt to suspension growth naturally and conduct transformation reversibly between the adherent and suspension modes. This culture model was confirmed to be susceptible to different fatal aquatic viruses and suitable for gene engineering as well. As a suspension culture system with no need for microcarriers and special additives, ES cells may be useful for the development of new aquatic serum-free production systems in a bioreactor or become a promising tool for the aquatic vaccine industry.

Abstract: Suspension growth can greatly increase the cell density and yield of cell metabolites. To meet the requirements of aquatic industries, a culture model derived from *Anguilla anguilla* skin was developed using the explant outgrowth and enzyme-digesting passaging methods. These cells were kept in vitro continuously for over 12 months and subcultured 68 times. This heteroploid cell line, designated as ES, can naturally adapt to adherent and suspension growth reversibly under certain temperatures, serum percentages, and inoculum densities, without the need for any microcarriers or special medium additives. The ES cells can continue being highly productive under a temperature range of 15–37 °C and a serum percentage ranging from 3 to 15%. An inoculum density higher than 5×10^5 cells·mL^{-1} is necessary for the ES cells to turn into suspension efficiently. The green fluorescent protein (GFP) reporter gene was successfully expressed in the ES cells. The ES cells demonstrated susceptibility to Anguillid herpesvirus (AngHV) and red-spotted grouper nervous necrosis virus (RGNNV). ES is the first natural suspension growth model of aquatic origin; it does not require the processes of suspension domestication and carrier dissolution, making it a promising and cost-effective model for vaccine production, bio-pharmaceutical manufacturing, and cellular agriculture.

Keywords: *Anguilla anguilla*; suspension growth; reversible adherent–suspension culture system; Anguillid herpesvirus; red-spotted grouper nervous necrosis virus

check for updates

Citation: Zheng, Z.; Chen, B.; Liu, X.; Guo, R.; Chi, H.; Chen, X.; Pan, Y.; Gong, H. Novel Eel Skin Fibroblast Cell Line: Bridging Adherent and Suspension Growth for Aquatic Applications Including Virus Susceptibility. *Biology* **2024**, *13*, 1068. https://doi.org/10.3390/biology13121068

Academic Editor: Roy Ambli Dalmo

Received: 25 November 2024
Revised: 15 December 2024
Accepted: 18 December 2024
Published: 20 December 2024

Copyright: © 2024 by the authors. Licensee MDPI, Basel, Switzerland. This article is an open access article distributed under the terms and conditions of the Creative Commons Attribution (CC BY) license (https://creativecommons.org/licenses/by/4.0/).

1. Introduction

Cells cultivated in suspension play an important role in the massive production of vaccines, biopharmaceuticals, and cell-based foods [1–4]. However, only a few mammalian cell lines currently meet the industrial requirements of stable growth in suspension, including Baby Hamster Kidney (BHK) cells, Chinese Hamster Ovary (CHO) cells, Human Embryonic Kidney 293 (HEK293) cells, and Madin Canine Kidney (MDCK) cells [5–8]. To develop more suspension culture models, various methods have been attempted to enable adherent cells to grow in suspension since the 1960s, such as using a special culture medium, long-term adaptation/domestication, or genetic engineering [9–13]. As for aquatic research, there is no aquatic cell line considered as versatile as CHO or Vero simian kidney epithelial (Vero) cells in the vaccine industry [14–16]. Because almost all known teleost somatic cell lines are adherent [17] and mammalian suspension culture systems are insensitive to many aquatic viruses, the absence of suspension culture models of aquatic origin has facilitated the application of some adherent cell lines in aquatic vaccine production, although with relatively lower efficiency. For example, Epithelioma Popuasum cuprini (EPC) cells are commonly used in spring viremia of carp virus (SVCV) vaccines [18,19], and Mandarin Fry fin type-I (MFF-1) cells were used in the development of Infectious Spleen and Kidney Necrosis Virus (ISKNV) vaccines [20]. To increase the efficiency and scale of the manufacturing of aquatic vaccines and other cell-based products, the development of an aquatic-origin suspension culture system is urgently needed.

Many freshwater eels of Anguillidae are wildly cultured as species for food consumption, and East Asia is the center of the global eel industry. In the late 1990s and the first decade of this century, *Anguilla anguilla* was the most productive species of the eel culture industry in China [21]. In 2009, *A. anguilla* was listed as CR (critically endangered) by the International Union for Conservation of Nature (IUCN), and *A. anguilla* has ceased to be the leading species of the Chinese eel industry since an exportation prohibition of glass eels took effect in 2010. Studies on *A. anguilla* cell lines are worthwhile to enhance the protection of stock and prevention of diseases in all Anguillidae members. The three most important viral pathogens of *A. anguilla* are eel virus European (EVE), eel virus European X (EVEX), and Anguillid herpesvirus (AngHV), all of which are commonly detected in the skin of infected eels and cause festering. Furthermore, these viruses have been reported to infect other aquaculture Anguillidae species, such as *Anguilla japonica* and *Anguilla rostrata* [21–23], implying that an *A. anguilla* skin cell line could be applied in the manufacturing of vaccines from various Anguillidae species. There were several cell lines that originated from Anguillidae species before 2006, and none of them were created from *A. anguilla* [24]. In 2007, our lab began a series of research studies on cell and tissue culture from the target organs of eels, including the kidney, liver, fin, skin and muscles, and several *A. anguilla* cell lines have been established successfully to form a small, single-species-derived cell bank [24–27].

In the present study, to build an efficient in vitro culture model for virus isolation and vaccine development using *Anguilla* sp., a new *A. anguilla* skin cell line, ES, was established and characterized. A long-term time-course growth observation was conducted using batch culture and simulated semi-continuous culture processes to determine the suspension features of the ES cell line, demonstrating its advantages as a natural reversible adherent–suspension culture model. The infection tests confirmed its susceptibility to both AngHV and red-spotted grouper nervous necrosis virus (RGNNV), two important aquatic viruses in the Chinese aquaculture industry. The ES cell line shows potential for the production of aquatic vaccines and other cell-based protein products.

2. Materials and Methods

2.1. Cell Line Development and Authentication

2.1.1. Primary Culture and Subculture

The explant outgrowth method was applied to initiate the primary culture [28]. Healthy *A.anguilla* elvers with an average weight of 2 g were over-anesthetized using

20 mg/L of 3-aminobenzoic acid ethyl ester methane sulfonate (Sigma-Aldrich, St. Louis, MO, USA) and then disinfected 3 times with 2% iodine tincture and 75% alcohol. The mucus layer was removed entirely. Fresh skin tissues were excised and cut into 1 mm^3 pieces, rinsed with ice-cold 0.01 mol/L PBS containing 200 IU·mL^{-1} of penicillin (Sangon, Shanghai, China) and 200 μg·mL^{-1} of streptomycin (Sangon, Shanghai, China) 3 times, and then attached to the inner face of a 25 cm^2 culture flask (Corning Inc., Corning, NY, USA) coated with Leibovitz's L-15 medium (Basalmedia, Shanghai, China). The primary culture was carried out at 26 °C with 5 mL of L-15 containing 15% fetal bovine serum (Oricell, Guangzhou, China) and antibiotics, among which 2 mL was applied after attachment, while the other 3 mL was added in 3 batches equally during 72 h. A full medium change was carried out every 72 h. After 20 d in vitro, the primary culture was digested with a 0.25% trypsin-0.02% EDTA solution (Procell, Wuhan, China) at 26 °C for 5 min and then centrifuged for 3 min at 1500 rpm. The cell suspension was prepared with 5 mL of the full culture medium and inoculated into a new 25 cm^2 culture flask incubated at 26 °C until a confluent cell monolayer was observed.

In accordance with our previous studies [24,27], 50 continuous subcultures were carried out with a split ratio of 1:2 to build a cell line, which was characterized to grow in suspension naturally at higher passages. For cells of different passages, the subculture conditions are listed in Table 1; in particular, cells grown in suspension should be collected along with the supernatant and purified via an extra centrifugation step before digestion. For cryopreservation, the *A. anguilla* skin cells were harvested and diluted to a density of 10^6 cells·mL^{-1} following 24 to 48 h of growth in vitro and stored in liquid nitrogen (−196 °C) through a routine programmed cooling procedure. The cryopreservation medium was made up of 70% L-15, 20% FBS, and 10% dimethyl sulfoxide (DMSO) (Sigma-Aldrich, St. Louis, MO, USA). Four weeks post cryopreservation, a recovery–viability examination was conducted using the trypan blue method [29].

Table 1. The subculture parameters of eel skin (ES) cells.

Cell State [A/S]	Cell Passage [d]	Digestion Time [s]	Centrifuge Speed [rpm]	Centrifuge Time [min]	FBS [%]	Interval [h]
Adherent	2–20	60	1500	3	15	24–48
Adherent	21–50	30–45	1800	5	10	24
Adherent	>50	30–45	1800	5	8	24
Suspension	>50	300	1800	5	8	96–168

2.1.2. 18S rRNA Sequence Analysis

The origin of the ES cells was authenticated using 18s recombinant (r) RNA gene sequencing [30]. The total genomic DNA of passage 53 ES cells was extracted using the FastPure Blood/Cell/Tissue/Bacteria DNA Isolation Mini Kit (Vazyme, Nanjing, China). A pair of specific primers, namely, *18S-F/R* (Table 2), was designed according to the published total *A. anguilla* 18s rRNA sequence (GenBank accession No. FM946070.1) [31]. The polymerase chain reaction (PCR) amplification system was composed of a 50 μL reaction mix containing 25.0 μL of Taq Master Mix (Vazyme, Nanjing, China), 2.0 μL of each primer (10 μM each), and 1 μL of DNA templates. The PCR conditions were as follows: initial denaturation at 94 °C for 3 min, 30 cycles at 94 °C for 30 s, 55 °C for 1.5 min, and 72 °C for 1 min, with a final elongation at 72 °C for 10 min. The PCR products were analyzed via agarose electrophoresis and a gel imaging system (Thermo Nanodrop 2000, Waltham, MA, USA). The recovered DNA products were purified and sequenced by Sangon Biotech Co., Ltd. (Shanghai, China).

Table 2. The PCR primers used in this study.

Primer Name	Forward Sequence (5′-3′)	Reverse Sequence (5′-3′)
18s-F/R	TATGCTTGTCTCAAAGATTAAGCCATGC	CACCTACGGAAACCTTGTTACGA
HVA F/R	TTGAGGTTGTTGTCGTGCC	CTCTCATGTCATCCAGACGG
HVA pol F/R	GTGTCGGGCCTTTGTGGTGA	GTGTCGGGCCTTTGTGGTGA
VNN F2/R3	CGTGTCAGTCATGTGTCGCT	CGAGTCAACACGGGTGAAGA

2.1.3. Chromosome Analysis

According to our previous research [24], following 36 h in vitro, passage 50 ES cells were treated with 1 μg·mL^{-1} colchicine (Sigma-Aldrich, St. Louis, MO, USA) for 5 h. The cells were then harvested and suspended in 0.3% KCl solution. After the hypotonic treatment for 25 min, a 3-step fixation procedure with Carnoy's fixative solution (methanol/acetic acid = 3:1, 0 °C) was conducted for 5 min at room temperature, 10 min at room temperature, and overnight at 4 °C. The fixed cells were dripped on ice-cold slides and air dried, and they were then stained with 10% Giemsa. The karyotypes of 100 metaphase cells were photographed (Eclipse TE2000-S, Nikon Instruments Inc., Tokyo, Japan) and analyzed following a classic protocol [32].

2.1.4. Immuno-Cytochemical Identification

To identify the cell type of the ES cells, an immunofluorescent analysis was carried out [31]. The ES cells at passage 55 were planted on cover slips (Corning Inc., Corning, NY, USA) and transferred to a 6-well plate for 24 h at a density of 2 × 10^5 cells·mL^{-1} and fixed with 4% paraformaldehyde (Servicebio, Wuhan, China) overnight at 4 °C before staining. The antibodies used are listed in Table 3, and the cell nuclei were marked with DAPI (Servicebio, Wuhan, China). The labeled cells were observed using an ECLIPSE TI confocal microscope (Nikon Instruments Inc., Tokyo, Japan).

Table 3. Antibodies for immunofluorescent identification.

Antibody	Type	Source
Acidic cytokeratin	Monoclonal mouse	Servicebio, Wuhan, China
Basic cytokeratin	Monoclonal mouse	Servicebio, Wuhan, China
Collagen-1	Monoclonal mouse	Servicebio, Wuhan, China
Desmin	Monoclonal mouse	Servicebio, Wuhan, China
Fibronectin	Monoclonal mouse	Servicebio, Wuhan, China
Vimentin	Monoclonal mouse	Servicebio, Wuhan, China
Fluorescein isothiocyanate (FITC) conjugated	Goat anti-mouse IgG	Servicebio, Wuhan, China

2.2. Growth Characterization

A long-term observation of the growth characteristics of the ES cells was carried out in a batch culture process. Passage 54 ES cells were inoculated into 250 mL culture flasks at a density of 5 × 10^5 cells·mL^{-1} and incubated in L-15 medium supplemented with 10% FBS. Continuous micrography was conducted for 16 d (Eclipse TE2000-S, Nikon, Nikon Instruments Inc., Tokyo, Japan). At 4 d, 8 d, and 12 d following inoculation, the suspension ratio and the major axis of the cell clusters were measured and compared; the cell clusters in suspension were finally collected and subcultured into new flasks at the same density after thorough digestion (Table 1). Another 16 d observation was carried out in a simulated semi-continuous culture process. At 4 d, 8 d, and 12 d following inoculation, the cells in suspension were removed and accompanied by a full medium change, and the secondary growth of the adherent parts was then recorded and evaluated.

The growth curves of the ES cells were plotted at passage 55. With an interval of 24 h, the average adherent cell density and suspension cell density of different groups were measured separately using a hemocytometer (n = 3). The cell population doubling time

(PDT) was determined using the formula below (where T means the population doubling time of the logarithmic phase, N_t represents the final number of cells, N_0 represents the initial number of cells, and t represents the time interval between N_t and N_0) [33] as follows:

$$T = t\,[\lg 2\,(\lg N_t - \lg N_0)^{-1}]. \quad (1)$$

The purified ES cells were diluted to two densities of 2×10^5 cells·mL^{-1} and 10^6 cells·mL^{-1} and then inoculated into 50 mL flasks and calculated. The serial tests based on the serum percentage and temperature differences were blocked in the 2×10^5 cells·mL^{-1} group due to the absence of suspension cells (26 °C, 10% FBS). The 10^6 cells·mL^{-1} samples were incubated and measured as follows: at 26 °C, five groups of ES cells were incubated in L-15 medium supplemented with 3%, 5%, 8%, 10%, and 15% FBS; subsequently, the second batch of five groups was kept in L-15 medium containing 8% FBS and incubated at 15 °C, 20 °C, 26 °C, 30 °C, and 37 °C; and finally, the growth curves of the adherent and suspension cells were plotted. The ratios between the suspension cell numbers and the total cell numbers (%) of each group at 72 h, 120 h, and 168 h were analyzed and compared.

2.3. Cell Transfection

The ES cells at passage 50 were inoculated in a 6-well culture plate (Corning Inc., Corning, NY, USA) with a density of 10^6 cells·mL^{-1}. After being incubated at 26 °C for 24 h, the cells were transfected with the GFP reporter gene carrier pEGFP-N1 (Biomed, Beijing, China) using a lipofectamine™ 3000 kit (Invitrogen, Carlsbad, CA, USA). According to the official protocol with some modifications, the working diluent contained 2.5 μg of pEGFP-N1 plasmid, 5 μL of lipofectamine™ 3000 reagent, and 250 μL of minimum essential medium (MEM) (Gibco, New York City, NY, USA). The transfected cells were observed and visualized via fluorescence microscopy (Eclipse TE2000-S, Nikon, Nikon Instruments Inc., Tokyo, Japan) every 24 h, and the transfection efficiency was evaluated based on the ratio of green fluorescence-positive cells to all cells in 10 distinct optical fields.

2.4. Susceptibility Test

The ES cells were infected with 2 aquatic viruses, namely, RGNNV and AngHV. The ES cells (passage 50) inoculated at a density of 5×10^5 cells·mL^{-1} were first incubated at 26 °C for 18–24 h to form a confluent monolayer and then transferred to the maintenance medium (L-15 containing 3% FBS) at 30 °C at 4 h prior to infection. The viral samples were prepared with the supernatant from RGNNV-infected EPC cells and AngHV-infected EL cells [24,34] and then added to the ES cells (200 μL per flask). The infected cells were observed under a phase-contrast microscope (Eclipse TE2000-S, Nikon, Nikon Instruments Inc., Tokyo, Japan) continuously to access cytopathic effects (CPEs). A subculture was carried out every 7 days or after reaching a cytopathic rate of over 60%. The infected cell number was estimated by counting the living cells using a flow cytometer (BD Accuri™, Becton, Dickinson and Co., Franklin Lakes, NJ, USA) and compared with the control group.

After 3 subcultures, total DNA was extracted as PCR templates from the infected cells using a FastPure Blood/Cell/Tissue/Bacteria DNA Isolation Mini Kit (Vazyme, Nanjing, China) at 96 h post-infection. The PCR detection of RGNNV was conducted with a pair of specific primers, namely, *VNN F2/R3* (Table 2) [35], while identification for AngHV was conducted with two pairs of specific primers, namely, *HVAF/R* and *HVApolF/polR* (Table 2) [36,37].

2.5. Data Analysis

Each experiment was repeated at least three times. The data are shown as mean ± standard deviation (SD), and statistical significance was determined via multiple comparisons within the framework of one-way analysis of variance (ANOVA, Turkey's HSD test) [33] using GraphPad Prism 9.5 (www.graphpad.com, accessed on 31 July 2024).

2.6. Electron Microscopy

At 48 h post-infection, the infected ES cells were pre-fixed with 2.5% glutaraldehyde in cacodylate buffer (0.1 M, pH 7.4) for 1 min and then harvested and suspended in 2.5% glutaraldehyde for 4 h at room temperature (25–28 °C). After centrifugation at 1000 rpm for 2 min, the precipitate was incubated in 2.5% glutaraldehyde overnight at 4 °C [38]. Ultrathin sectioning and transmission electron microscopy (TEM) were subsequently conducted by Servicebio Technology Co., Ltd. (Wuhan, China).

3. Results

3.1. Cell Line Establishment and Authentication

3.1.1. Primary Cell Culture and Cell Line Establishment

Following inoculation, the cells migrated outwards from the explants within 48 h, and radial outgrowths covered over 70% of the area of the flask's inner surface in 2 weeks (Figure 1a). After the first digestion, subcultures were performed at an interval of approximately 24 h continuously (split ratio = 1:2). At passage 20, the cell strain was purified and demonstrated fibroblast-like fully adherent cells (Figure 1b). The eel skin (ES) cell line was subcultured over 60 times in vitro and usually maintained in L-15 containing 8% FBS at 26 °C (Figure 1c). The ES cells recovered from liquid nitrogen storage at the 60th subculture reached confluency within 3 days; their average viability was evaluated to be over 80% (Figure 1d).

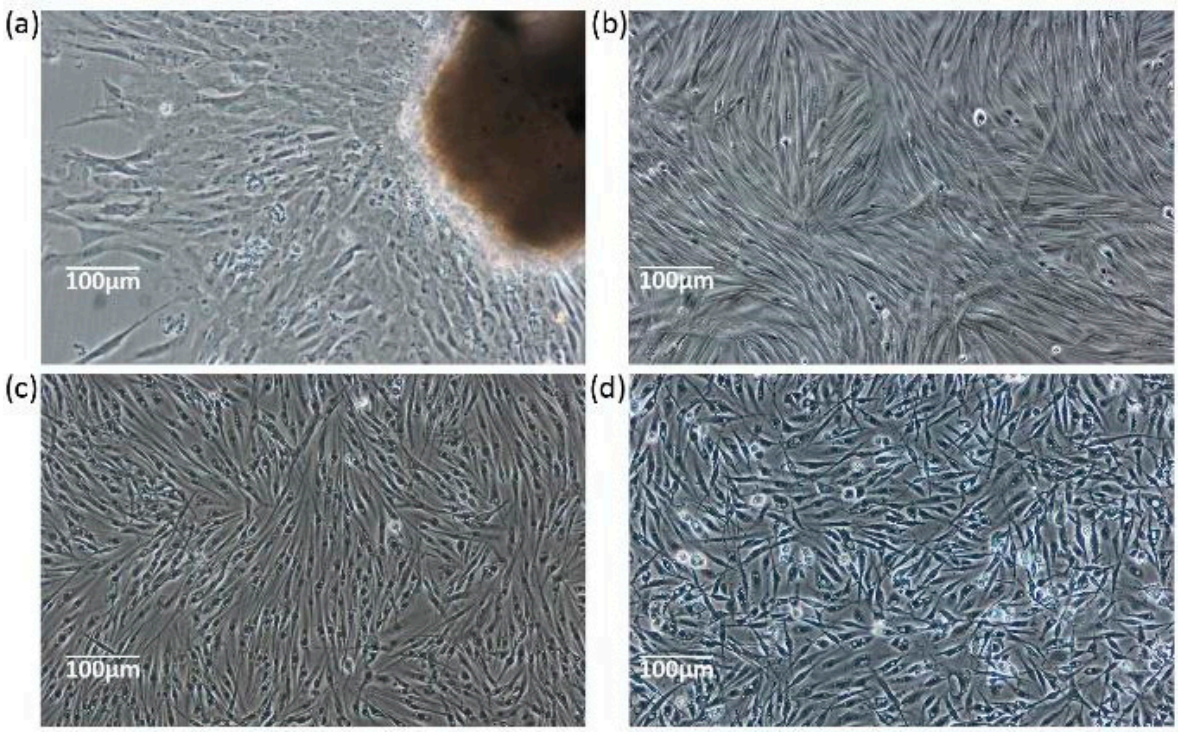

Figure 1. Development of the ES cell line. (**a**) Primary culture of *A. anguilla* skin; (**b**) passage 20 ES cells; (**c**) passage 55 ES cells at 24 h in vitro; and (**d**) passage 60 ES cells at 72 h post recovery from liquid nitrogen.

3.1.2. 18S rRNA Sequence Analysis

The origin of the ES cells was authenticated via 18S rRNA gene analysis. Using the specific pair of primers *18S-F/R* (Table 2), an expected product of 1714 bp was amplified and sequenced, which was 100% identical to the published *A. anguilla* 18S rRNA sequence (GenBank: FM946070.1). These results confirmed that the ES cells derived from *A. anguilla* were kept uncontaminated during passaging.

3.1.3. Chromosome Analysis

A total of 100 metaphase ES cells (passage 50) were analyzed; their chromosome number ranged from 18 to 96 (Figure 2a). The modal diploid karyotype of $2n = 38$ was presented in only 15% of all samples, suggesting that the ES cell line was aneuploid (Figure 2b) [39].

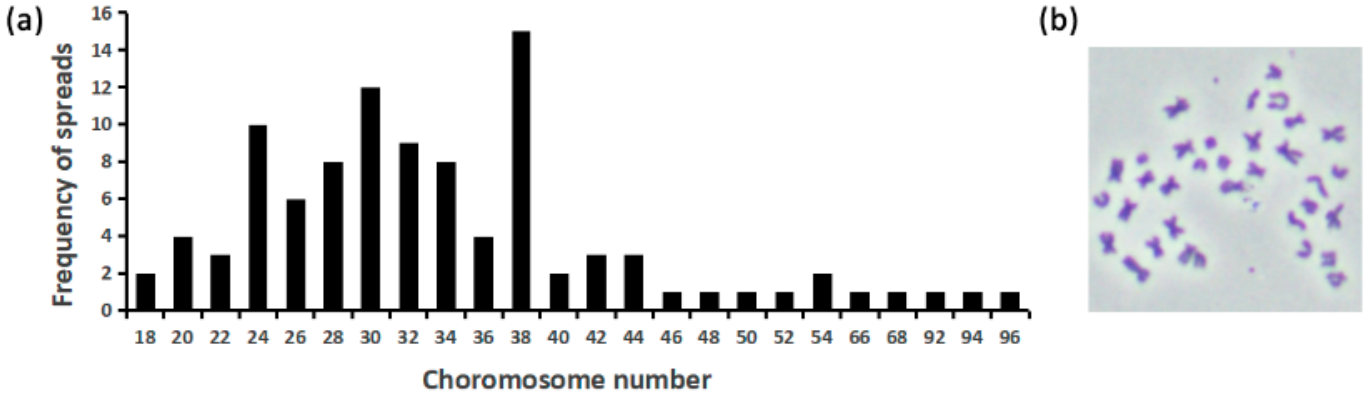

Figure 2. Chromosome analysis of ES cells at passage 50. (**a**) The distribution of chromosome number, among which only 15% of samples ($n = 100$) presented a diploid karyotype ($2n = 38$). (**b**) The metaphase of a typical aneuploidy ES cell.

3.1.4. Immuno-Cytochemical Identification

To determine the nature of the ES cells, five kinds of cell markers were identified with six monoclonal antibodies, as described in Table 3. The fluorescent signals were observed to be strongly positive for the vimentin and desmin groups (Figure 3a,b), moderately positive for the fibronectin and collagen-1 group (Figure 3d,e), and negative for the cytokeratin group (Figure 3c). Vimentin and desmin were globally expressed in the cytoplasm (Figure 3a,b); however, fibronectin and collagen-1 were distributed at the cell surface with punctate agglomerations (Figure 3d,e). These results suggested that the ES cell line was fibroblastoid [40].

3.2. Growth Characterization

3.2.1. Batch Culture Process and Simulated Semi-Continuous Culture Process

In the batch culture process with an inoculum density of 5×10^5 cells·mL^{-1}, a confluent monolayer was formed by day 2; spheroidal cell clusters were first observed to be adherent and then automatically turned into suspension over time with volume increases. In the meantime, co-localized attraction and disintegration of the adherent cell layer occurred along with the presence of suspending cell clusters (Figure 4a). The suspension ratio and volume change in the cell clusters at different stages were measured and analyzed (Figure 4e). On day 4, all cell clusters were attached to the surface of the cell layer, with their major axis ranging from 48.42 to 81.09 μm; on day 8, the adherent and suspension clusters shared a major axis ranging from 127.22 to 221.75 μm; and by day 12, all clusters observed were in suspension with a major axis in the range of 135.38–355.04 μm, while the adherent cells were still observed to be in a dispersed pattern (Figure 4a,e).

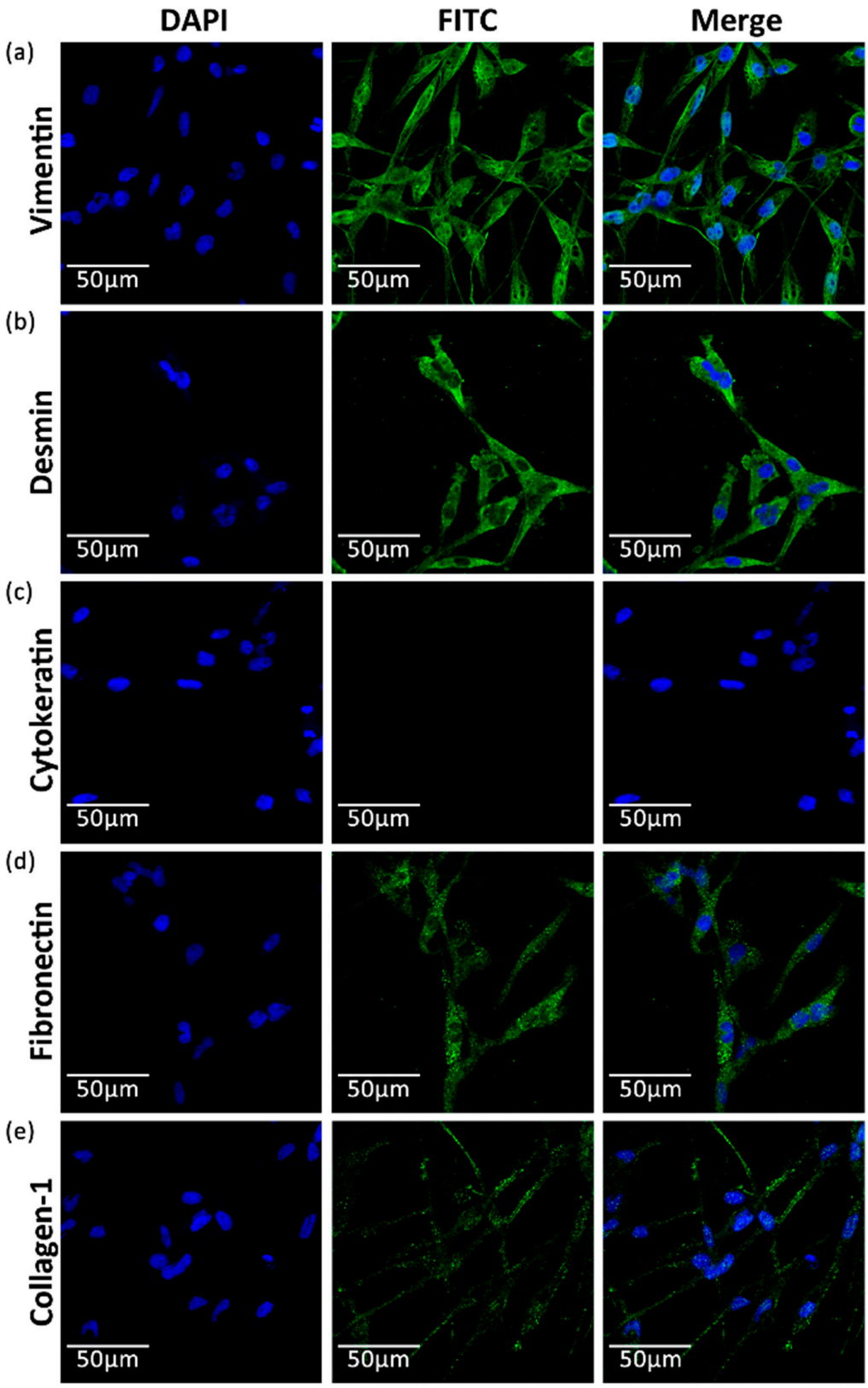

Figure 3. Immunofluorescence staining of 5 markers in passage 55 ES cells: (**a**) vimentin; (**b**) desmin; (**c**) cytokeratin; (**d**) fibronectin; and (**e**) collagen-1. The cell nuclei are indicated with DAPI (blue), and the cell markers are indicated with FITC (green).

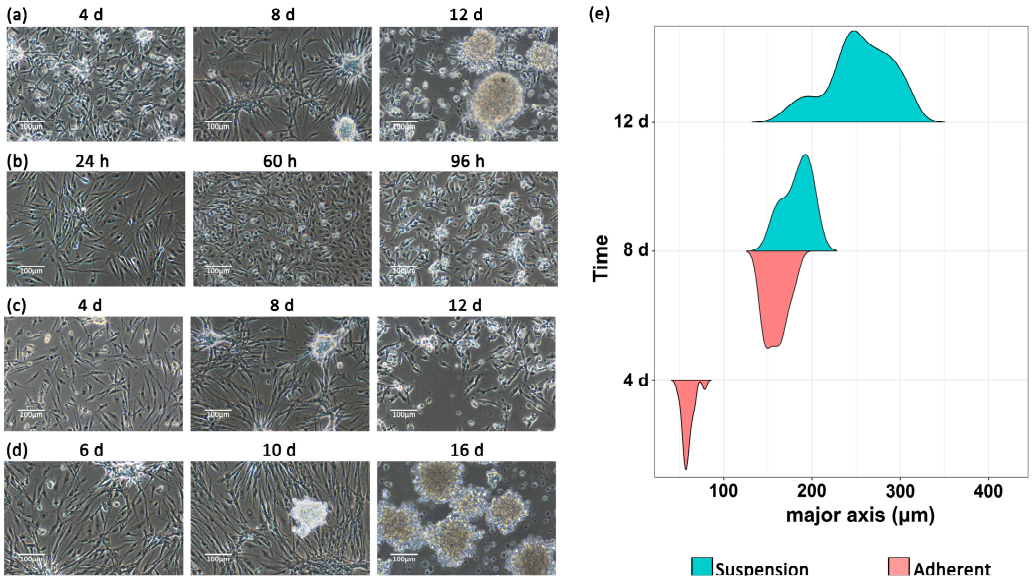

Figure 4. Passage 54 ES cells in a batch culture process and a simulated semi-continuous culture process. (**a**) The autonomous formation of suspension cell clusters; (**b**) the re-formation of cell clusters after digestion; (**c**) the harvest of suspension cells with a full medium change; (**d**) the compensation of adherent cell-layer lesions and output of new suspension cell clusters; (**e**) the violin plots of the adherent/suspension ratio and the major axis of the cell clusters over a 12 d long-term observation.

For the cell clusters that were collected and thoroughly digested, the natural process from being completely adherent to cluster formation was reproduced exactly within 96 h post-re-inoculation (Figure 4b), and subsequent observations confirmed the replication of an autonomous suspension. These results suggested that the ES cells can form a biphasic culture system, switching between the adherent and suspension modes reversibly (Figures 4, S2 and S3).

In the semi-continuous culture process simulated in the flasks, at the time points of day 4 and day 8 after all culture medium and suspension cells were removed (Figure 4c), the adherent cells succeeded in compensating the lesion inflicted by cluster formation and reconstructed a confluent cell layer (Figure 4d); at the time point of day 12, the new cells were overwhelmingly agglomerated in suspension (Figure 4c,d). These results indicated the potential of ES cells to reach higher production limits than those obtained using a simple batch culture process.

3.2.2. Growth Characteristics

When inoculated at a low density of 2×10^5 cells·mL^{-1}, the suspension growth of the ES cells was inhibited significantly, and the total growth curve and the adherent growth curve almost coincided. From 48 to 120 h following inoculation, the ES cells (passage 55) were found in the logarithmic phase with a PDT of 35.46 h (Figure S1).

At an inoculum density of 10^6 cells·mL^{-1}, the ES cells became completely attached and formed a confluent monolayer at all five serum percentages tested (Figure S2). The highest growth rate, the ratio of suspension cells to the total number of cells, and the number of cell clusters in suspension were all positively correlated with the serum percentage (Figures 5a,c and S2). In particular, there were suspension cells, which dispersed in the 3% group and formed no clusters (Figure S2a). From 48 to 144 h after inoculation, the adherent cells were observed to first move into the logarithmic growth phase and then form a second growth peak following the increase in the suspension growth rate (Figure 5a), suggesting probable compensatory effects for the cell-layer lesions inflicted by the transposition of cell clusters into suspension; in the groups subjected to high FBS percentages (8%, 10% and 15%), the suspension cells surpassed the adherent cells to be the major population in vitro

(Figures 5a and S2c–e). The highest adherent growth rate was measured in the 8% group, while the maximum suspension growth rate was recorded in the 10% group (Figure 5a,c).

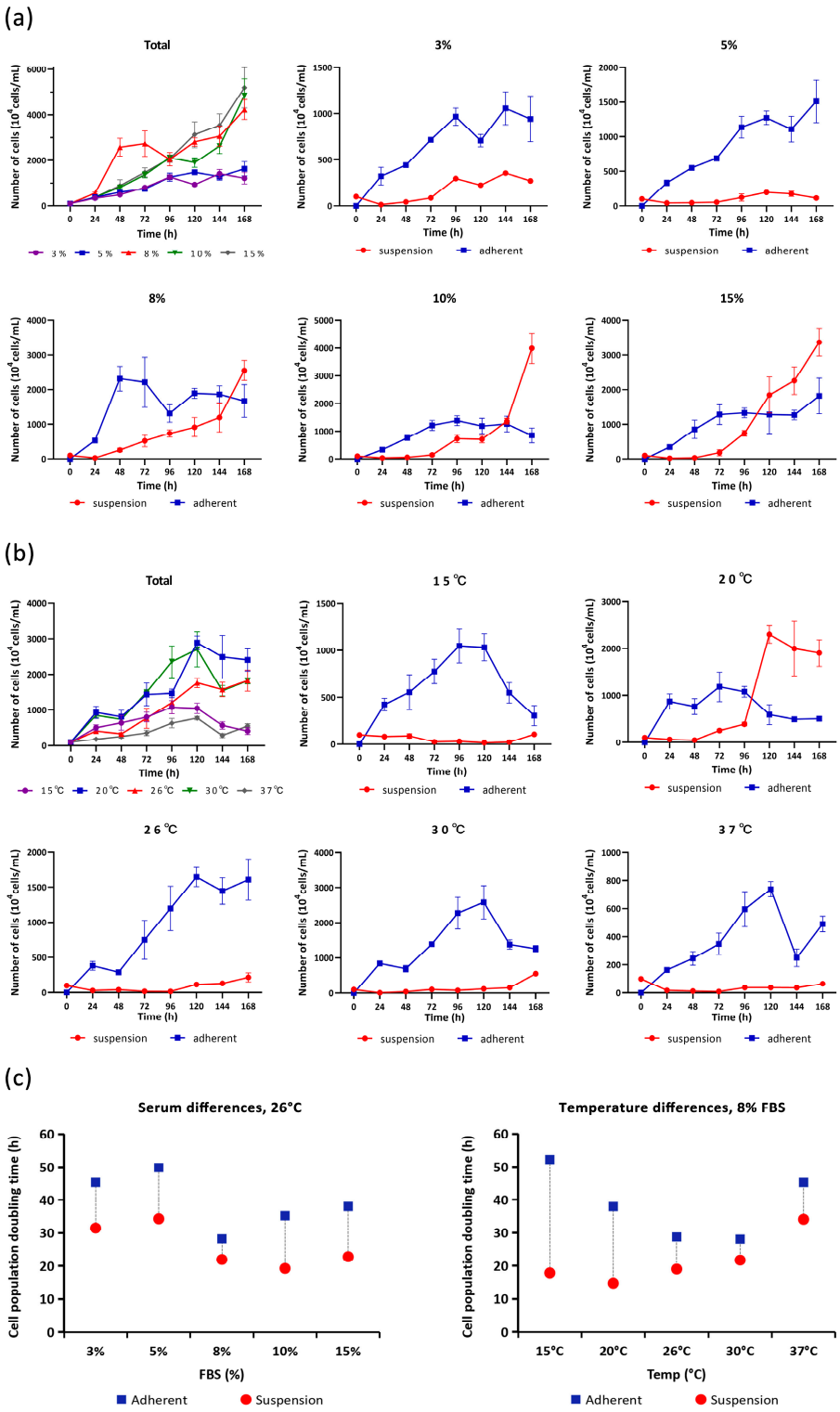

Figure 5. The growth characteristics of passage 55 ES cells under different serum percentages and temperatures. (**a**) Growth curves at 26 °C with different FBS%; (**b**) growth curves at different temperatures with 8% FBS (inoculum density = 10^6 cells·mL^{-1}); and (**c**) the population doubling time (PDT) of adherent and suspension cells. The growth curve values are exhibited as the mean ± standard deviation (SD), $n = 3$.

When inoculated at a density of 10^6 cells·mL^{-1}, the ES cells became fully attached and continued being highly productive at a temperature range from 15 to 37 °C. At 15 °C, a delayed attachment at 48 h was observed, and the subsequent cell growth pattern was network like (Figure S3a); at the other four temperatures tested, the ES cells finished attachment within 24 h and succeeded in forming a confluent monolayer. Suspension cell clusters were observed only in the three hypothermal–mesothermal groups (15 °C, 20 °C, and 26 °C) (Figure S3a–c), while all suspension cells were presented in a dispersed pattern at 30 °C and 37 °C (Figure S3d,e). A significant increase in cell volume was observed at 37 °C (Figure S3e). The logarithmic growth phase was plotted within the interval of 48 to 144 h following inoculation; the highest adherent growth rate was measured in the 30 °C group, while the maximum suspension growth rate was recorded in the 20 °C group (Figures 5b,c and S3b,d).

In the serum difference tests, at 72 h after inoculation, the suspension ratio (%) of the cells showed no significant difference among the five groups; at 120 h post-inoculation, the only significant difference was observed between the 3% and 5% groups; and at 168 h after inoculation, the suspension ratios of the 3% and 5% groups were significantly lower than those of the 8%, 10%, and 15% groups, while the suspension ratio of the 10% group was significantly higher than that of the 15% group (Figure 6a). In the temperature difference tests, the suspension ratio (%) of the 20 °C group was significantly higher than those of the other four groups at all time points. In addition, at 72 h after inoculation, the suspension ratio (%) of the 30 °C group was significantly higher than that of the 37 °C group; at 120 h post-inoculation, the suspension ratio (%) of the 15 °C group was significantly lower than those of the 26 °C, 30 °C, and 37 °C groups; and at 168 h after inoculation, the suspension ratio of the 30 °C group was significantly higher than those of the 26 °C and 37 °C groups (Figure 6b).

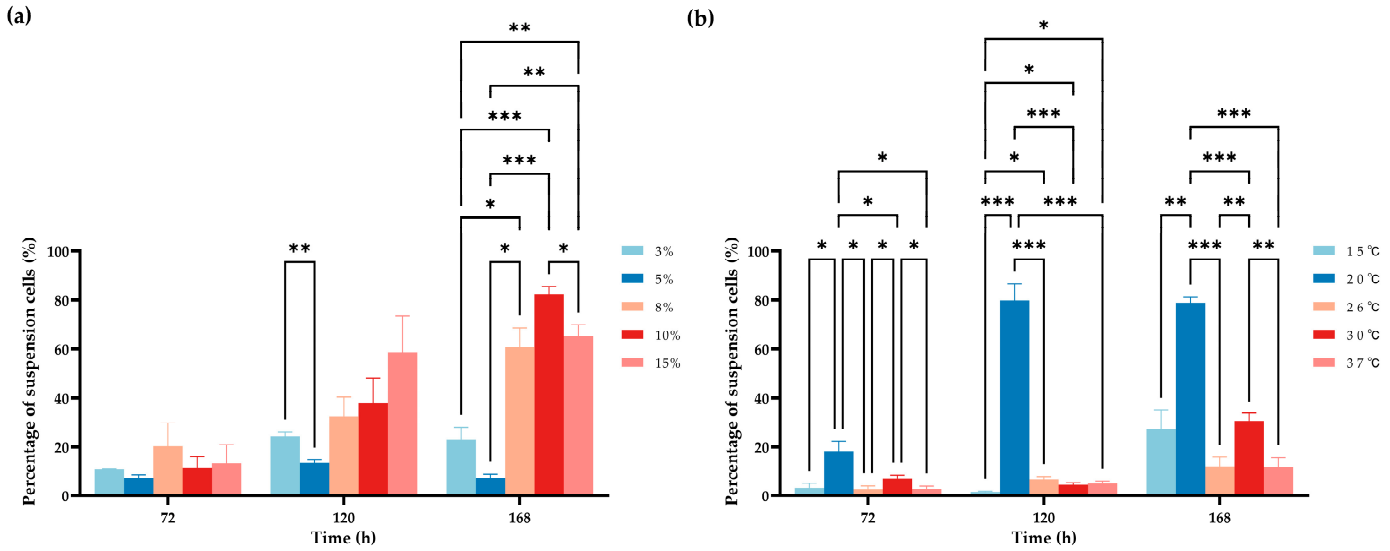

Figure 6. Analysis of the suspension ratio (%) of passage 55 ES cells under different serum percentages and temperatures. (**a**) Multiple comparisons at 26 °C with different FBS%; (**b**) multiple comparisons at different temperatures with 8% FBS (inoculum density = 10^6 cells·mL^{-1}). * $p < 0.05$, ** $p < 0.01$ and *** $p < 0.001$; $n = 3$.

From these results, we optimized the subculture conditions for the ES cells as follows: a temperature of 26 °C and 8% FBS (PDT = 29.81 h) and an inoculum density higher than 5×10^5 cells·mL^{-1} would be essential if suspension growth was expected. The maintenance culture conditions for virus infection were optimized as follows: a temperature of 30 °C and 3% FBS, with which the ES cells could form a confluent cell layer within 24 h and keep it for over 14 d.

3.3. Cell Transfection

Green fluorescent signals were first detected at 24 h following transfection and lasted for at least 96 h. At 48 h post-transfection, the transfection efficiency of pEGFP-N1 was measured to be about 10% (Figure 7).

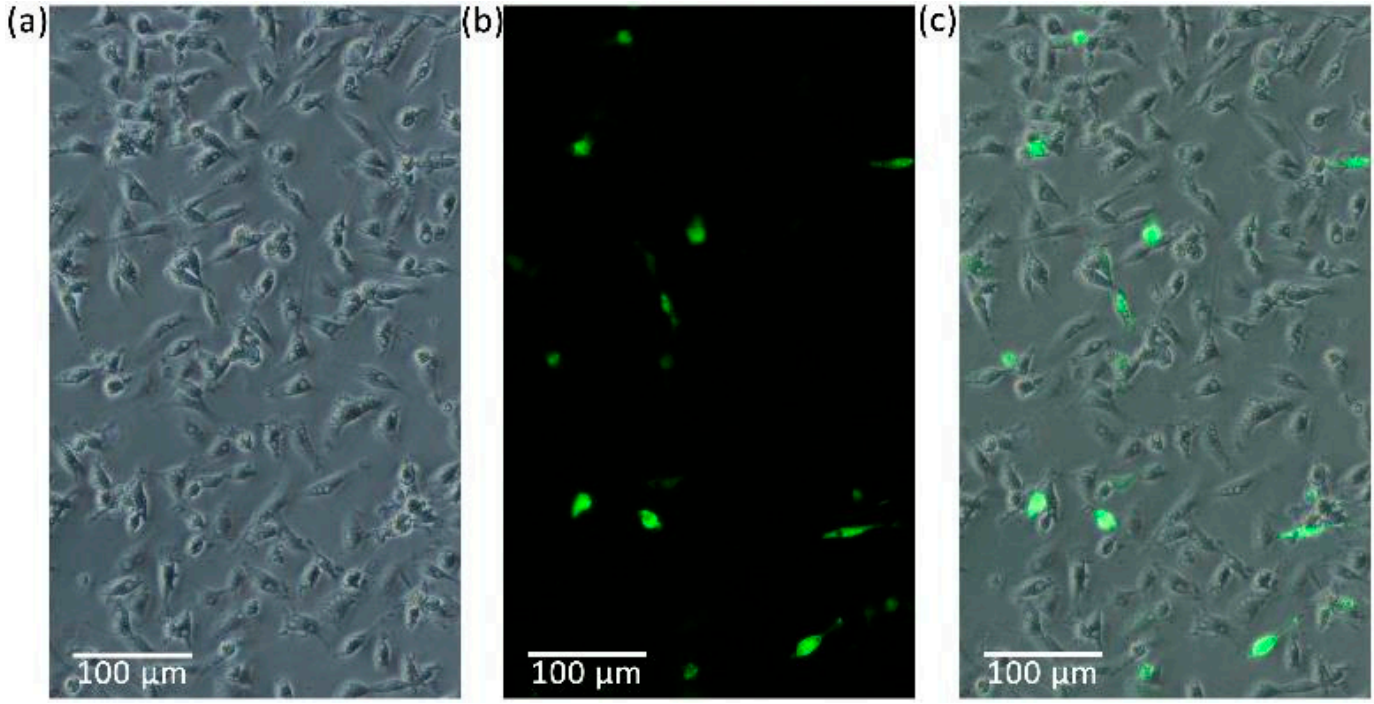

Figure 7. Passage 50 ES cells transfected with pEGFP-N1 for 48 h. (**a**) An optical micrograph; (**b**) a green fluorescence micrograph; and (**c**) a merging of the optical and GFP graphs.

3.4. Susceptibility Tests

Both the AngHV and RGNNV samples were able to cause CPEs on the ES cells continuously across the three subcultures. Compared with the confluent control groups (Figure 8a,c), the AngHV-infected cells were observed to have become rounded and detached from the monolayer at 60 hpi (hours post-infection) (Figure 8b), while the RGNNV-infected cells were observed to have shrunk and collapsed massively, accompanied by an increase in mortality. At 72 hpi, the mortality rate of the RGNNV-infected group was evaluated to be over 85% (Figure 8d).

The particles of both viruses were determined and found in the cytoplasm using an electron microscopy assay. Viral factories (VFs) with a lower electron density than that of the surrounding cytoplasm were present in the AngHV-infected cells [41], sheltering numerous empty capsids and immature viral particles inside, while mature virions were localized outside (Figure 8e). As for the RGNNV-infected cells, viral particles of different ages were all found dispersed in the cytoplasm (Figure 8f).

Following PCR amplification of the AngHV *pol* gene, the expected 390 and 622 bp products were readily detected (Figure S4a) [42]; for the RGNNV-positive samples, a 420–431 bp product was also detected via a standard viral nervous necrosis (VNN) diagnostic assay (Figure S4b) [35].

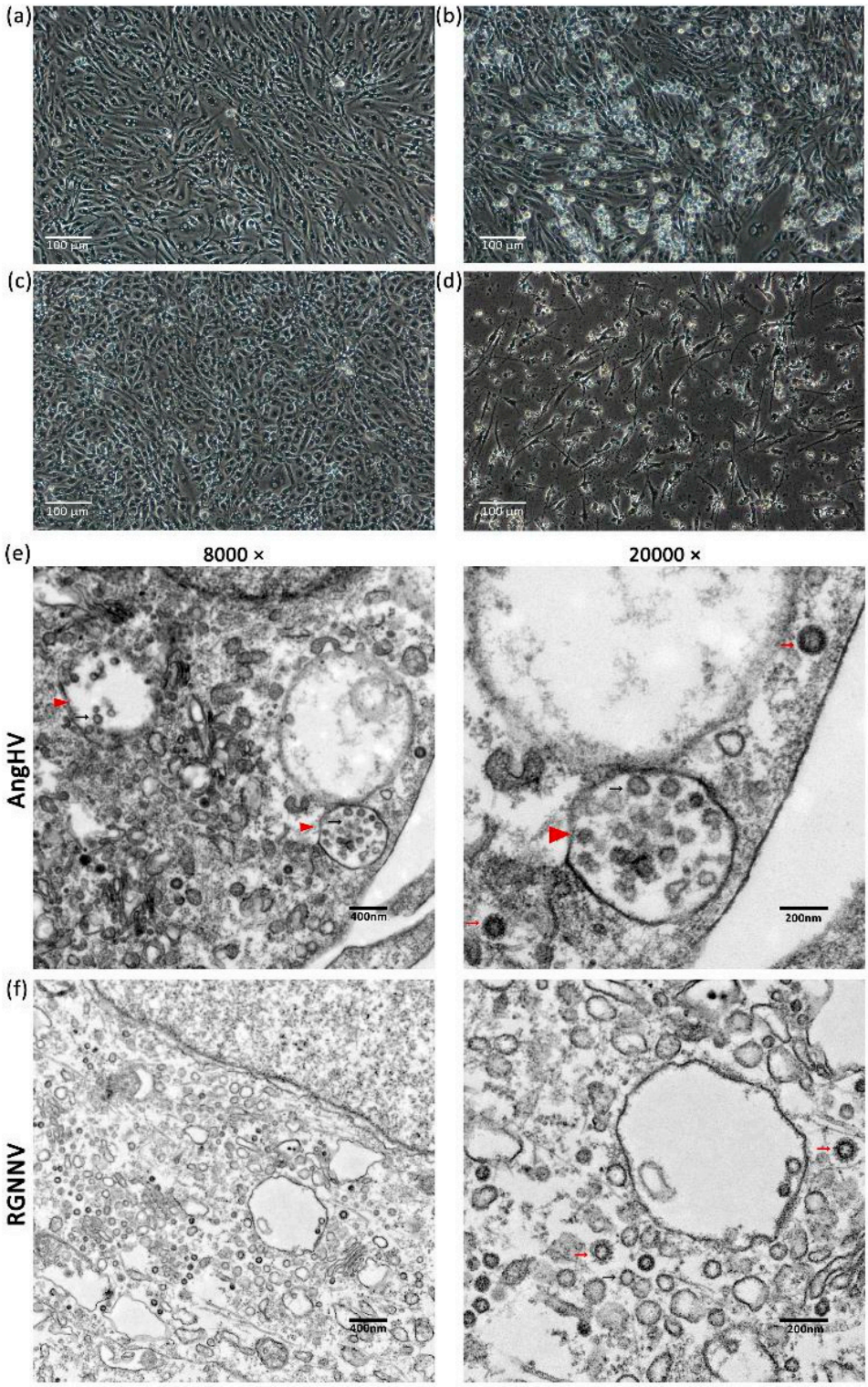

Figure 8. Susceptibility tests of passage 54 ES cells to two aquatic viruses. (**a**) The control group at 60 h in vitro; (**b**) ES cells infected with Anguillid herpesvirus (AngHV), 3 subcultures at 60 hpi; (**c**) the control group at 72 h in vitro; (**d**) ES cells infected with red-spotted grouper nervous necrosis virus (RGNNV), 3 subcultures at 72 hpi; (**e**) an electron microscopic image of AngHV particles inside infected ES cells at 48 h post-infection; (**f**) an electron microscopic image of RGNNV particles inside infected ES cells at 48 h post-infection. Red triangles indicate viral factories (VFs) with a low electron density; small red arrows indicate mature viral particles; small black arrows indicate immature viral particles.

4. Discussion

In the last 20 years, fish cell culture has been weaning itself off the heritage of mammalian techniques. Over 90% of new cell lines originated from fish have turned to wide-temperature CO_2-free culture models based on Leibovitz's L-15 medium, which has abolished the ventilation system and made the culture procedure more compact and cost effective [17,43,44]. Furthermore, the high recovery ratio of ES cells cryopreserved in a single-cell suspension has been authenticated (Figure 4), while rapid freezing–thawing is also used in in vitro adaptation of stem cell differentiation and organoid induction [45–47]. Developing a cryopreservation procedure for ES cells as suspension clusters may be a viable idea to increase productivity further. Therefore, a suspension cell culture model from fish represents a combination of a stable environment, high cell density, and easy expansion.

The ES cells were found to induce a naturally conditioned suspension growth pattern in the batch culture process, which could be modulated by adjusting routine culture parameters, including initial inoculum density, serum percentage, and temperature. To optimize the subculture protocol, both the adherent and suspension applications were taken into consideration. According to Table 1, the 96–168 h interval of purified suspension cells is too long for small-scale experiments; therefore, the adherent subculture methods were chosen. To observe the adherent–suspension transformation of ES cells quickly, a minimum inoculum density of 5×10^5 cells·mL^{-1} is suggested (Figures 4 and S1). In the re-inoculation test of the counted cells on day 7 (26 °C, 8% FBS), an inoculum density over 2×10^7 cells·mL^{-1} resulted in full suspension within 96 h. The optimum density and cycle for suspension ES cells on a large scale should probably be measured with a high lower limit [3]. A low serum percentage inhibited the natural initiation of suspension growth (Figures 5 and S1). Especially, in the 3% FBS batch culture process, the ES cells could be maintained for over 2 weeks at a density of 10^7 cells·mL^{-1}, which implied the tolerance of the ES cells to an oligotrophic environment and the further possibility for serum-free culture adaptation [48]. At all time points analyzed, the active suspension growth of the ES cells at 20 °C as cell clusters was remarkable (Figures 5 and 6b). In their very early life stages with a culture temperature limit of 16–22 °C, the expression patterns of the *A. anguilla* larval genes *gh* and *igf-1* were reported to be delayed at 16 °C but accelerated at 20–22 °C [49]. Investigating the regulation of these genes may help in understanding the selective preference of suspension ES cells for a certain temperature window. In all batch culture tests, the PDT of the suspension cells was measured to be shorter than that of the adherent cells from the same sample (Figure 5c), suggesting the potential for high biomass yield in a purified suspension culture. At 26 °C and 8% FBS, the maximum growth rate of adherent and suspension cells came to a minimum distance (Figure 5c), and the cell suspension ratio (%) presented the least significant differences among the multiple comparisons (Figure 6); from passage 55–68, the ES cells were maintained stably with this subculture protocol, confirming its convenience.

The ES cells were found to present susceptibility to multiple aquatic viruses. AngHV is the most threatening viral pathogen for Anguillidae members, and it has been found in most aquaculture areas in Asia and Europe [23,37,50–55], as well as in wild silver eels from the migrating populations [56]. *A. anguilla* prefers a culture temperature range of 18–26 °C, while other Anguillidae commercial species, which are all AngHV sensitive, can adapt to higher culture temperatures of up to 30 °C [21]. Since 2008, our lab has developed a series of cell lines that originated from different tissues of *A. anguilla* to study AngHV [24–27]. AngHV-infected syndromes are mainly shown in the skin, gills, kidney, liver, and spleen. Compared with previous infection samples at 20–26 °C using viscera cell lines [24,57], the ES infection model presented typical CPEs rapidly at 30 °C, which accords with the water temperature during the epidemic season in Fujian and Guangdong province, the main eel culture-producing areas in China, suggesting that the ES cell line can be a universal model for AngHV vaccine production from Anguillidae members.

In addition to AngHV, the ES cells also exhibited susceptibility to RGNNV, which was once detected in cultured *A. anguilla* in Taiwan [58], but it is not a usual pathogen of farmed

Anguilla rostrata and *Anguilla marmorata* in recent years; its relative, the striped jack nervous necrosis virus (SJNNV), was observed being carried by wild eels of Spain [59]. At present, RGNNV is predominant worldwide, with grouper (*Epinephelus* sp.) and European sea bass (*Dicentrarchus labrax*) as the most susceptible victim species [34]. Our results implicated VNN as a threat in abeyance for cultured eels and offered a new potential culture system for RGNNV vaccine production.

As a traditionally popular economic species, *A. anguilla* is now critically endangered due to overfishing, environmental pollution, hydrological change, and diseases [21]. Being listed in Appendix II of the Convention on International Trade in Endangered Species of Wild Fauna and Flora (CITES), *A. anguilla* has conceded its leading place in the Chinese eel industry to *A. rostrata* and *A. marmorata* since the exportation prohibition of glass eels in 2010 [60]. Because of their special catadromous life cycle [61], the failure of artificial reproduction, and the catch-depending aquaculture mode, the abundance of many Anguillidae species in their original habitat is decreasing every year [62]. Research studies on *A. anguilla* are worthwhile to enhance the protection of stock and prevention of diseases in all Anguillidae members. Furthermore, culturing cell lines originating from edible parts, such as the skin and muscles, may bring the unique flavor of *A. anguilla* back to the table through cell-based food production via in vitro organoid induction and mass bioreactor production [63–65]. ES cells' suspension feature places them well in the competition of cellular agriculture and, it is a viable tool to preserve the genetic resources of endangered eels.

5. Conclusions

In conclusion, an aneuploid cell line from ES (eel skin) was developed as the first aquatic culture system that can naturally adapt to suspension culture. This fibroblastic culture system can be reversibly converted between the adherent and suspension modes, and it can reach a high cell density of a magnitude of 10^7 cells·mL^{-1} easily without the need for special additives or microcarriers. The ES cells can be transfected with foreign reporter genes and are sensitive to multiple important aquatic viruses. All these results suggest that the ES culture system is more cost effective by removing the processes of suspension domestication and carrier dissolution, which can benefit the production of aquatic vaccines, biopharmaceutics, or cellular agriculture.

Supplementary Materials: The following supporting information can be downloaded at https://www.mdpi.com/article/10.3390/biology13121068/s1, Figure S1: ES cells cultured at a low inoculum density; Figure S2: ES cells cultured under different FBS percentages; Figure S3: ES cells cultured under different temperatures; Figure S4: PCR tests of the susceptibility of ES cells.

Author Contributions: Conceptualization, Z.Z.; methodology, Z.Z.; software, X.L. and Y.P.; validation, Z.Z. and H.C.; formal analysis, Z.Z., X.L., Y.P. and X.C.; investigation, Z.Z., B.C. and H.C.; resources, R.G. and H.G.; data curation, Z.Z.; writing—original draft preparation, Z.Z.; writing—review and editing, Z.Z and H.G.; visualization, X.L. and Z.Z.; supervision, H.G.; project administration, H.G.; funding acquisition, H.G., Z.Z. and X.C. All authors have read and agreed to the published version of the manuscript.

Funding: The present study was supported by the National Key Research and Development Program of China (Grant no. 2022YFD2401002 to H.G.), the Project of Local Science and Technology Development Guided by the Central Government (Grant no. 2023L3024 to X.C.), the Youth Project of Fujian Academy of Agricultural Sciences (Grant no. A2007QJ06 to Z.Z.) and the Key Project of Fujian Academy of Agricultural Sciences (Grant no. KJZD202402 to X.C.).

Institutional Review Board Statement: This study was conducted in accordance with the Declaration of Helsinki and was approved by the Laboratory Animal Bioethics Committee of the Biotechnology Institute, Fujian Academy of Agricultural Sciences (Approval No. BI-AEC-0007055002, May 2007; BI-AEC-20230208, February 2023).

Informed Consent Statement: Not applicable.

Data Availability Statement: The data that support the findings of this study are available from the corresponding author upon reasonable request.

Conflicts of Interest: The authors declare no conflicts of interest.

References

1. Gregersen, J.P.; Schmitt, H.J.; Trusheim, H.; Broker, M. Safety of MDCK Cell Culture-Based Influenza Vaccines. *Future Microbiol.* **2011**, *6*, 143–152. [CrossRef]
2. Ryu, N.; Lee, S.; Park, H. Spheroid Culture System Methods and Applications for Mesenchymal Stem Cells. *Cells* **2019**, *8*, 1620. [CrossRef] [PubMed]
3. Vlecken, D.H.; Pelgrim, R.P.; Ruminski, S.; Bakker, W.A.; van der Pol, L.A. Comparison of Initial Feasibility of Host Cell Lines for Viral Vaccine Production. *J. Virol. Methods* **2013**, *193*, 28–41. [CrossRef] [PubMed]
4. Waltz, E. No Bones, No Scales, No Eyeballs: Appetite Grows for Cell-Based Seafood. *Nat. Biotechnol.* **2021**, *39*, 1483–1485. [CrossRef]
5. Kretzmer, G. Industrial Processes with Animal Cells. *Appl. Microbiol. Biotechnol.* **2002**, *59*, 135–142. [CrossRef] [PubMed]
6. Kildegaard, H.F.; Baycin-Hizal, D.; Lewis, N.E.; Betenbaugh, M.J. The Emerging CHO Systems Biology Era: Harnessing the 'Omics Revolution for Biotechnology. *Curr. Opin. Biotechnol.* **2013**, *24*, 1102–1107. [CrossRef]
7. Grieger, J.C.; Soltys, S.M.; Samulski, R.J. Production of Recombinant Adeno-Associated Virus Vectors Using Suspension HEK293 Cells and Continuous Harvest of Vector from the Culture Media for GMP FIX and FLT1 Clinical Vector. *Mol. Ther.* **2016**, *24*, 287–297. [CrossRef] [PubMed]
8. Zhang, J.; Qiu, Z.; Wang, S.; Liu, Z.; Qiao, Z.; Wang, J.; Duan, K.; Nian, X.; Ma, Z.; Yang, X. Suspended Cell Lines for Inactivated Virus Vaccine Production. *Expert. Rev. Vaccines* **2023**, *22*, 468–480. [CrossRef]
9. Capstick, P.B.; Telling, R.C.; Chapman, W.G.; Stewart, D.L. Growth of a Cloned Strain of Hamster Kidney Cells in Suspended Cultures and their Susceptibility to the Virus of Foot-and-Mouth Disease. *Nature* **1962**, *195*, 1163–1164. [CrossRef]
10. Chu, C.; Lugovtsev, V.; Golding, H.; Betenbaugh, M.; Shiloach, J. Conversion of MDCK Cell Line to Suspension Culture by Transfecting with Human Siat7e Gene and its Application for Influenza Virus Production. *Proc. Natl. Acad. Sci. USA* **2009**, *106*, 14802–14807. [CrossRef] [PubMed]
11. Lee, N.; Shin, J.; Park, J.H.; Lee, G.M.; Cho, S.; Cho, B.K. Targeted Gene Deletion Using DNA-Free RNA-Guided Cas9 Nuclease Accelerates Adaptation of CHO Cells to Suspension Culture. *ACS Synth. Biol.* **2016**, *5*, 1211–1219. [CrossRef]
12. van Wielink, R.; Kant-Eenbergen, H.C.; Harmsen, M.M.; Martens, D.E.; Wijffels, R.H.; Coco-Martin, J.M. Adaptation of a Madin-Darby Canine Kidney Cell Line to Suspension Growth in Serum-Free Media and Comparison of its Ability to Produce Avian Influenza Virus to Vero and BHK21 Cell Lines. *J. Virol. Methods* **2011**, *171*, 53–60. [CrossRef] [PubMed]
13. Moran, M.J.; Chen, J.; Piret, J.M.; Balcarcel, R.R. Super7 Passaging Method to Improve Chinese Hamster Ovary Cell Fed-Batch Performance. *Biotechnol. Bioeng.* **2024**, *121*, 3068–3075. [CrossRef] [PubMed]
14. Ozaki, H.; Govorkova, E.A.; Li, C.; Xiong, X.; Webster, R.G.; Webby, R.J. Generation of High-Yielding Influenza a Viruses in African Green Monkey Kidney (Vero) Cells by Reverse Genetics. *J. Virol.* **2004**, *78*, 1851–1857. [CrossRef]
15. Tihanyi, B.; Nyitray, L. Recent Advances in CHO Cell Line Development for Recombinant Protein Production. *Drug Discov. Today Technol.* **2020**, *38*, 25–34. [CrossRef]
16. Sanchez-Martinez, Z.V.; Alpuche-Lazcano, S.P.; Stuible, M.; Durocher, Y. CHO Cells for Virus-Like Particle and Subunit Vaccine Manufacturing. *Vaccine* **2024**, *42*, 2530–2542. [CrossRef]
17. Kumar, M.S.; Singh, V.K.; Mishra, A.K.; Kushwaha, B.; Kumar, R.; Lal, K.K. Fish Cell Line: Depositories, Web Resources and Future Applications. *Cytotechnology* **2024**, *76*, 1–25. [CrossRef] [PubMed]
18. Embregts, C.; Rigaudeau, D.; Tacchi, L.; Pijlman, G.P.; Kampers, L.; Vesely, T.; Pokorova, D.; Boudinot, P.; Wiegertjes, G.F.; Forlenza, M. Vaccination of Carp Against SVCV with an Oral DNA Vaccine or an Insect Cells-Based Subunit Vaccine. *Fish. Shellfish. Immunol.* **2019**, *85*, 66–77. [CrossRef]
19. Guo, S. Construction and Evaluation on Immune Effect of Biomimetic Cell-Derived Vaccine Delivery System against Spring Viremia of Carp. Master's Thesis, Northwest A&F University, Xianyang, China, 2022.
20. Fu, Y.; Li, Y.; Zhang, W.; Fu, W.; Li, W.; Zhu, Z.; Weng, S.; He, J.; Dong, C. Effectively Protecting Asian Seabass *Lates calcarifer* from ISKNV-I, ISKNV-II, RSIV-II and SDDV by an Inactivated ISKNV-I and SDDV Bivalent Vaccine. *Aquaculture* **2023**, *566*, 739218. [CrossRef]
21. Kaifu, K.; Stein, F.; Dekker, W.; Walker, N.; Dolloff, C.A.; Steele, K.; Aguirre, A.A.; Nijman, V.; Siriwat, P.; Sasal, P. Global Exploitation of Freshwater Eels (Genus Anguilla): Fisheries, Stock Status and Illegal Trade. In *Eels Biology, Monitoring, Management, Culture and Exploitation, Proceedings of the First International Eel Science Symposium, Sheffield, UK, 31 October 2019*, 1st ed.; Don, A., Coulson, P., Eds.; 5m Publishing: Sheffield, UK, 2019; Volume 6, Chapter 23, pp. 377–422. [CrossRef]
22. Haenen, O.; van Ginneken, V.; Engelsma, M.; van den Thillart, G. Impact of Eel Viruses on Recruitment of European Eel. In *Spawning Migration of the European Eel*; van den Thillart, G., Dufour, S., Rankin, J.C., Eds.; Springer: Dordrecht, The Netherlands, 2009; pp. 387–400. [CrossRef]
23. Ueno, Y.; Kitao, T.; Aoki, T.; Chen, S.N.; Kou, G.H. Characterization of a Herpes-like Virus Isolated from Cultured Japanese Eels in Taiwan. *Gyobyo Kenkyu* **1992**, *27*, 7–17. [CrossRef]

24. Zheng, Z.; Yang, J.; Ge, J.; Chi, H.; Chen, B.; Fang, Q.; Gong, H. Development and Characterization of a Continuous Cell Line (EL) from the Liver of European Eel *Anguilla anguilla*. *Cell Biol. Int.* **2020**, *44*, 808–820. [CrossRef]
25. Mao, N.; Zheng, Z.Y.; Lin, T.L. The Growth Advantage of the Pectoral Fin Cells of *Angailla anguilla* Under Different Culture Conditions. *Fujian J. Agric. Sci.* **2012**, *27*, 222–226. [CrossRef]
26. Mao, N.; Zheng, Z.Y.; Chen, S.Y. Growth Factors, bFGF and IFG-1, in Pectoral Fin Passage Cells of *Anguilla anguilla*. *Fujian J. Agric. Sci.* **2012**, *27*, 578–582. [CrossRef]
27. Chen, B.; Zheng, Z.; Yang, J.; Chi, H.; Huang, H.; Gong, H. Development and Characterization of a New Cell Line Derived from European Eel *Anguilla anguilla* Kidney. *Biol. Open* **2019**, *8*, bio037507. [CrossRef] [PubMed]
28. Bryson, S.P.; Joyce, E.M.; Martell, D.J.; Lee, L.E.; Holt, S.E.; Kales, S.C.; Fujiki, K.; Dixon, B.; Bols, N.C. A Cell Line (HEW) from Embryos of Haddock (*Melanogrammus aeglefinius*) and its Capacity to Tolerate Environmental Extremes. *Mar. Biotechnol.* **2006**, *8*, 641–653. [CrossRef]
29. Ott, T. Tissue Culture of Fish Cell Lines. In *NWFHS Laboratory Procedures Manual*, 2nd ed.; True, K., Ed.; U.S. Fish and Wildlife Service: Onalaska, TX, USA, 2004; Chapter 10, pp. 1–16. Available online: https://fws.gov/media/national-wild-fish-health-survey-laboratory-procedures-manual (accessed on 7 September 2011).
30. Frankowski, J.; Bastrop, R. Identification of *Anguilla anguilla* (L.) and *Anguilla rostrata* (Le Sueur) and their Hybrids Based on a Diagnostic Single Nucleotide Polymorphism in Nuclear 18S rDNA. *Mol. Ecol. Resour.* **2010**, *10*, 173–176. [CrossRef]
31. Gong, J.; Huang, Y.; Huang, X.; Ouyang, Z.; Guo, M.; Qin, Q. Establishment and Characterization of a New Cell Line Derived from Kidney of Grouper, *Epinephelus akaara* (Temminck & Schlegel), Susceptible to Singapore Grouper Iridovirus (SGIV). *J. Fish. Dis.* **2011**, *34*, 677–686. [CrossRef] [PubMed]
32. Levan, A.; Fredga, K.; Sandberg, A.A. Nomenclatrue for Centromeric Position on Chromosomes. *Hereditas* **1964**, *52*, 201–220. [CrossRef]
33. Davis, J.M. *Basic Cell Culture: A Practical Approach*, 2nd ed.; Oxford University Press: New York, NY, USA, 2002; pp. 200–226.
34. Bandin, I.; Souto, S. Betanodavirus and VER Disease: A 30-Year Research Review. *Pathogens* **2020**, *9*, 106. [CrossRef] [PubMed]
35. Chen, A.P.; Zhang, L.F.; Wang, S.; Gao, L.Y.; Jiang, Y.L.; Chen, X.Z.; Zhu, Z.W.; Jing, H.L. *PRC Aquatic Industry Standard: Diagnostic Protocol for Fish Viral Nervous Necrosis, SC/T 7216-2012*; Ministry of Agriculture of the People's Republic of China: Beijing, China, 2012; pp. 2–4.
36. Shih, H.H. A Polymerase Chain Reaction for Detecting *Herpesvirus anguillae* in Asymptomatic Eels. *Taiwania* **2004**, *49*, 1–6.
37. Ge, J.Q.; Yang, J.X.; Gong, H.; Lin, T.L. Isolation and Identification of a Herpesvirus from Cultured European Eels *Anguilla anguilla* in China. *J. Fish. China* **2014**, *38*, 1579–1583. [CrossRef]
38. Zhao, Z.; Li, F.; Ning, J.; Peng, R.; Shang, J.; Liu, H.; Shang, M.; Bao, X.Q.; Zhang, D. Novel Compound FLZ Alleviates Rotenone-Induced PD Mouse Model by Suppressing TLR4/MyD88/NF-kappaB Pathway through Microbiota-Gut-Brain Axis. *Acta Pharm. Sin. B* **2021**, *11*, 2859–2879. [CrossRef] [PubMed]
39. Yang, W.; Kuang, X.M.; Wang, J.; Xu, Y.M.; Guo, S. Comparison of Karyotypes of *Anguilla anguilla* and *Anguilla japonica*. *J. South China Agric. Univ.* **1999**, *20*, 47–50.
40. Vo, N.; Katzenback, B.A.; Kellendonk, C.; Duong, T.; Curtis, T.M.; Dixon, B.; Bols, N.C. Characterization of the Continuous Skin Fibroblastoid Cell Line, WE-skin11f, from Walleye (*Sander vitreus*). *J. Fish. Dis.* **2019**, *42*, 1587–1599. [CrossRef]
41. Zhang, Q.Y.; Gui, J.F. *Atlas of Aquatic Viruses and Viral Diseases*, 1st ed.; Science Press: Beijing, China, 2012; pp. 192–208.
42. van Beurden, S.J.; Bossers, A.; Voorbergen-Laarman, M.H.; Haenen, O.L.; Peters, S.; Abma-Henkens, M.H.; Peeters, B.P.; Rottier, P.J.; Engelsma, M.Y. Complete Genome Sequence and Taxonomic Position of Anguillid Herpesvirus 1. *J. Gen. Virol.* **2010**, *91*, 880–887. [CrossRef] [PubMed]
43. Lakra, W.S.; Swaminathan, T.R.; Joy, K.P. Development, Characterization, Conservation and Storage of Fish Cell Lines: A Review. *Fish. Physiol. Biochem.* **2011**, *37*, 1–20. [CrossRef] [PubMed]
44. Swaminathan, T.R.; Narendrakumar, L.; Prasannan Geetha, P.; Shanmuganathan, A.R.; Dharmaratnam, A.; Nithianantham, S.R. Comprehensive Update on Inventory of Finfish Cell Lines Developed during the Last Decade (2010–2020). *Rev. Aquacult* **2021**, *13*, 2248–2288. [CrossRef]
45. Altmaier, S.; Meiser, I.; Lemesre, E.; Chanrion, B.; Steeg, R.; Leonte, L.E.; Holst, B.; Nielsen, B.S.; Clausen, C.; Schmidt, K.; et al. Human iPSC-derived Hepatocytes in 2D and 3D Suspension Culture for Cryopreservation and In Vitro Toxicity Studies. *Reprod. Toxicol.* **2022**, *111*, 68–80. [CrossRef]
46. Magalhaes, R.; Nugraha, B.; Pervaiz, S.; Yu, H.; Kuleshova, L.L. Influence of Cell Culture Configuration on the Post-Cryopreservation Viability of Primary Rat Hepatocytes. *Biomaterials* **2012**, *33*, 829–836. [CrossRef]
47. Taylor, M.J.; Weegman, B.P.; Baicu, S.C.; Giwa, S.E. New Approaches to Cryopreservation of Cells, Tissues, and Organs. *Transfus. Med. Hemotherapy* **2019**, *46*, 197–215. [CrossRef] [PubMed]
48. Merten, O.W. Introduction to Animal Cell Culture Technology-Past, Present and Future. *Cytotechnology* **2006**, *50*, 1–7. [CrossRef]
49. Politis, S.N.; Mazurais, D.; Servili, A.; Zambonino-Infante, J.L.; Miest, J.J.; Sorensen, S.R.; Tomkiewicz, J.; Butts, I. Temperature Effects on Gene Expression and Morphological Development of European Eel, *Anguilla anguilla* Larvae. *PLoS ONE* **2017**, *12*, e182726. [CrossRef] [PubMed]
50. Chang, P.H.; Pan, Y.H.; Wu, C.M.; Kuo, S.T.; Chung, H.Y. Isolation and molecular characterization of herpesvirus from cultured European eels *Anguilla anguilla* in Taiwan. *Dis. Aquat. Organ.* **2002**, *50*, 111–118. [CrossRef]

51. Li, Y.Y.; Yang, J.X.; Chen, X.; Chen, Q.; Song, T.Y.; Ge, J.Q. Proteomic Profiling Skin Mucus of European Eel *Anguilla anguilla* Infected with Anguillid Herpesvirus. *Int. J. Mol. Sci.* **2022**, *23*, 11283. [CrossRef]
52. Motoaki, S.; Haruhiko, F.; Tokuo, S. Isolation and Characterization of a New Herpesvirus from Eel. In *Pathology in Marine Science*; Perkins, T.O., Cheng, T.C., Eds.; Academic Press: New York, NY, USA, 1990.
53. Ueno, Y.; Shi, J.W.; Yoshida, T.; Kitao, T.; Sakai, M.; Chen, S.N.; Kou, G.H. Biological and Serological Comparisons of Eel Herpesvirus in Formosa (EHVF) and *Herpesvirus anguillae* (HVA). *J. Appl. Ichthyol.* **1996**, *12*, 49–51. [CrossRef]
54. Kibenge, F.S.; Garate, O.N.; Johnson, G.; Arriagada, R.; Kibenge, M.J.; Wadowska, D. Isolation and Identification of Infectious Salmon Anaemia Virus (ISAV) from Coho Salmon in Chile. *Dis. Aquat. Organ.* **2001**, *45*, 9–18. [CrossRef]
55. van Nieuwstadt, A.P.; Dijkstra, S.G.; Haenen, O.L. Persistence of Herpesvirus of Eel *Herpesvirus anguillae* in Farmed European Eel *Anguilla anguilla*. *Dis. Aquat. Organ.* **2001**, *45*, 103–107. [CrossRef] [PubMed]
56. Lehmann, J.; Stürenberg, F.J.; Kullmann, Y.; Kilwinski, J. Umwelt-Und Krankheitsbelsatungen Der Aale in Nordrhein-Westfalen. *LÖBF-Mitteilungen* **2005**, *2*, 35–40.
57. Davidse, A.; Haenen, O.; Dijkstra, S.G.; Nieuwstadt, A.; Vorst, T.D.; Wagenaar, F.W.; Wellenberg, G.J. First Isolation of Herpesvirus of Eel (*Herpesvirus anguillae*) in Diseased European Eel (*Anguilla anguilla* L.) in Europe. *B Eur. Assoc. Fish. Pat.* **1999**, *19*, 137–141. [CrossRef]
58. Chi, S.C.; Shieh, J.R.; Lin, S.J. Genetic and Antigenic Analysis of Betanodaviruses Isolated from Aquatic Organisms in Taiwan. *Dis. Aquat. Organ.* **2003**, *55*, 221–228. [CrossRef]
59. Bandin, I.; Souto, S.; Cutrin, J.M.; Lopez-Vazquez, C.; Olveira, J.G.; Esteve, C.; Alcaide, E.; Dopazo, C.P. Presence of Viruses in Wild Eels *Anguilla anguilla* L., from the Albufera Lake (Spain). *J. Fish. Dis.* **2014**, *37*, 597–607. [CrossRef] [PubMed]
60. Wang, D.; Gao, H.Q.; Song, D.D.; Wu, F.X.; Li, Y.S.; Zhang, Y.X. *China Fishery Statistical Yearbook: 2024*, 1st ed.; Agriculture Press: Beijing, China, 2024; pp. 26–33.
61. Schmidt, J. Breeding Places and Migrations of the Eel. *Nature* **1923**, *111*, 51–54. [CrossRef]
62. Arai, T. Do we Protect Freshwater Eels or Do we Drive them to Extinction? *Springerplus* **2014**, *3*, 534. [CrossRef]
63. Goswami, M.; Belathur, S.Y.; Sathiyanarayanan, A.; Pinto, N.; Duscher, A.; Ovissipour, R.; Lakra, W.S.; Chandragiri, N.R. Cellular Aquaculture: Prospects and Challenges. *Micromachines* **2022**, *13*, 828. [CrossRef] [PubMed]
64. Ikeda, D.; Otsuka, Y.; Kan-No, N. Development of a Novel Japanese Eel Myoblast Cell Line for Application in Cultured Meat Production. *Biochem. Biophys. Res. Commun.* **2024**, *734*, 150784. [CrossRef] [PubMed]
65. Ovissipour, R.; Yang, X.; Saldana, Y.T.; Kaplan, D.L.; Nitin, N.; Shirazi, A.; Chirdon, B.; White, W.; Rasco, B. Cell-Based Fish Production Case Study for Developing a Food Safety Plan. *Heliyon* **2024**, *10*, e33509. [CrossRef]

Disclaimer/Publisher's Note: The statements, opinions and data contained in all publications are solely those of the individual author(s) and contributor(s) and not of MDPI and/or the editor(s). MDPI and/or the editor(s) disclaim responsibility for any injury to people or property resulting from any ideas, methods, instructions or products referred to in the content.